

Silicon surface passivation by PEDOT: PSS functionalized by SnO₂ and TiO₂ nanoparticles

M. García-Tecedor,^{a,b} S. Zh. Karazhanov,^{b,1} C. G. Vázquez,^{a,b} H. Haug,^b D. Maestre,^a A. Cremades,^a M. Taeño,^{a,c} M. J. Ramírez-Castellanos,^c J. M. González-Calbet,^c J. Piqueras,^a C. C. You,^b and E. S. Marstein^b

^a *Departamento de Física de Materiales, Facultad de CC. Físicas, Universidad Complutense, 28040, Madrid, Spain*

^b *Department for Solar Energy, Institute for Energy Technology (IFE), PO BOX 40, 2027, Kjeller, Norway*

^c *Departamento de Química Inorgánica I, Facultad de CC. Químicas, Universidad Complutense, 28040, Madrid, Spain*

ABSTRACT

Although rapid progress has been made on silicon-poly(3,4-ethylenedioxythiophene)/poly-(styrenesulfonate) (PEDOT:PSS) hybrid solar cells, one of the most important and challenging problem facing the technology is the understanding and control of the interface between the silicon (Si) substrate and the PEDOT:PSS material. In this paper, we present a systematic study of the passivation properties of the Si/PEDOT:PSS interface. We investigate both undoped PEDOT:PSS, as well as PEDOT:PSS functionalized with semiconducting oxide nanomaterials (TiO₂ and SnO₂). The hybrid compound was deposited at room temperature by spin coating, a potentially lower cost, process time and higher throughput alternative compared with the commonly used vacuum-based techniques. Photoluminescence imaging was used to characterize the electronic properties of the PEDOT:PSS/Si interface. Good surface passivation is achieved by PEDOT:PSS functionalized by the semiconducting oxides. We show that control of the concentration of semiconducting oxide nanoparticles in the polymer is

¹ Corresponding author: e-mail: smagulk@ife.no

crucial in determining the passivation performance. A charge carrier lifetime of about 275 μs has been achieved when using SnO_2 nanoparticles at a concentration of 0.5 wt.% as a filler in the composite film. X-Ray Diffraction (XRD), Scanning Electron Microscopy, High Resolution Transmission Electron Microscopy (HRTEM), Energy Dispersive X-Ray in a SEM, and μ -Raman Spectroscopy has been used for morphological, chemical and structural characterization. Finally, a photovoltaic device based on PEDOT:PSS functionalized with semiconducting oxide nanoparticles has been fabricated and the electrically characterized under both dark and illuminated conditions.

KEYWORDS: Silicon surface passivation, PEDOT:PSS, functionalization by SnO_2 or TiO_2 , hybrid material.

1. Introduction

The hybrid organic-Si solar cells are one group of emerging low cost and high efficiency photovoltaic (PV) devices, which combines the advantages of Si and organic PV technologies. The possibility to deposit an electrically conducting polymer by a chemical method at room temperature opened the possibility to use it as emitter layer, thus avoiding the added energy costs of the conventional emitter production process [1-2]. The most commonly used conductive polymer so far is poly(3,4-ethylenedioxythiophene)/poly-(styrenesulfonate) (PEDOT:PSS), which has a high *p*-type electrical conductivity, as well as good chemical stability and optical transparency in the visible range. An added advantage is that PEDOT:PSS can be easily processed in aqueous solution [3-5]. Within the last few years, efficiencies of Si-PEDOT:PSS hybrid cells have increased very fast, with reported efficiencies increasing from 12.3% [6] and 13% [7] in 2013 and 17.1 % [1] in 2014 to 18.3% and 20.3% [2] in 2015. If this trend can be continued, Si-PEDOT:PSS hybrid solar cells with efficiencies similar to the other most efficient Si solar cell technologies can be reached within a few years, potentially leading to a low cost route to high efficiency Si solar cells.

A key factor in determining the performance of a solar cell is the interface between components of the device characterized by interface states that can act as recombination centers for the charge carriers. It is therefore an important challenge to control the interface and develop an efficient method to passivate the Si surface [8], without adding additional large costs. While high efficiency Si-PEDOT:PSS solar cells have been developed successfully there are very few studies of interface properties.

At present, hydrogenated Si nitride ($\text{SiN}_x\text{:H}$), amorphous Si (a-Si), aluminum oxide (Al_2O_3) and silicon dioxide SiO_2 are the most well-known, successful inorganic materials used for Si surface passivation. However, these materials are processed either

using vacuum-based processes or at high temperatures. Additionally, pretreatment of Si surface with, e.g., hydrofluoric acid (HF) is usually required. Developing low temperature passivation methods and materials, involving simple procedure and low costs, is highly beneficial. Polymers have the potential to satisfy this requirement. These organic compounds can be deposited at room temperature and furthermore, upon processing at low temperatures, they can retain their main functionalities (see, e.g., Ref. [9]). The possibility of interface engineering has been also reported [7] by controlling the energy band offset that has led to the enhancement of the charge carrier lifetime. The use of polymers for Si surface passivation has therefore received increased attention recently in order to achieve a good solar cell performance [10]. As some examples, very poor Si surface passivation by PEDOT:PSS in 10.6% high efficiency Si/organic solar cells has been reported [11]. In some other works, high quality passivation of Si surface allowed [12] one to achieve surface recombination velocities below 10 cm/s. Passivation of Si surface by polymers other than PEDOT:PSS have also been considered in other works. In particular, poly(tetrafluoroethylene) based polymer Nafion[®] (DuPont) has been used [9] to achieve the surface recombination velocities of about 30 cm/s. Besides, it was reported in Ref. [13] that Si surface passivation has also been obtained for Si nanowire-based solar cells with a conversion efficiency of 10.2% using a similar approach. However, in these high efficiency Si-PEDOT:PSS solar cells [1] an advanced passivation scheme using an inorganic compound such as, e.g., SiO₂ has usually been applied. Amorphous Si has been used [10] between PEDOT:PSS and Si for surface passivation in ultrathin flexible planar Si cells. Formation of an inversion layer has been reported [14] between Si nanowires and PEDOT:PSS that suppresses the charge carrier recombination. The alcohol soluble polymer poly[(9,9-bis(3-(*N,N*-diethylamino)propyl)-2,7-fluorene)-*alt*-2,7-(9,9-dioctylfluorene)] has been also used [15] to improve Si/Al interface.

Recently composites made of PEDOT:PSS and inorganic nanostructures have been fabricated for different purposes. Synthesis of PEDOT:PSS-based hybrid compounds obtained by incorporating gold and silver nanoparticles has been reported [16-17] to enhance the plasmonic effect and to improve the electrical conductivity. In addition to metallic nanoparticles, semiconducting oxides nanoparticles have also been used in the formation of the composite. In particular, the fabrication of a PEDOT:PSS/tin oxide nanoparticle composite has been deposited [18] on glass substrate for anode applications. However, in order to eliminate water and other additives, thermal processing has been performed. Furthermore, due to the high amount of nanoparticles, low rotation speed of 400 r.p.m. is used during spin casting. As a result, grainy and several micron thick films are obtained composed by percolating SnO₂ nanoparticles. Hence, in that case, the resistivity of the film is reduced, and the valence band maximum and the Fermi level from PEDOT:PSS shifts correspondingly towards that of SnO₂. Fabrication of a composite material consisting of nanoparticles with a core of 25 nm size titanium oxide and a shell of PEDOT:PSS has also been developed [19] by using a technique based on a plasma treatment in aqueous solution. However, with that method a continuous and homogeneous composite thin film is not obtained. Another work on TiO₂ undoped nanoparticles/PEDOT:PSS composite has been published [20] in which nanoparticles smaller than 40 nm were dispersed into PEDOT:PSS in elevated weight ratios up to 20 wt.% to form a Schottky diode structure between aluminum and gold electrodes. The final thickness of the PEDOT:PSS/nanoparticle film is of 1 μm, presenting nano- and micro-size cracks depending on the final treatment. However, none of the above-mentioned papers reported on the passivation performance of the composite layer. The quality of the Si surface passivation strongly depends on PEDOT:PSS type used for deposition on Si. Although high-quality PEDOT:PSS passivates the Si surface well, it is very expensive.

Commonly, for deposition on top of Si, PEDOT:PSS has been functionalized by organic surfactants. It would be interesting to see, how the overall electronic and surface passivation properties of the PEDOT:PSS would depend on functionalization by inorganic nanomaterials.

In the present paper we investigate the surface passivation of Si substrates by use of bare PEDOT:PSS and PEDOT:PSS functionalized with either TiO₂ or SnO₂ nanoparticles. By including optimal concentrations of the nanomaterials we successfully obtain surface passivation as evidenced by charge carrier lifetimes of up to ~270 μs. This is a promising and competitive value considering that the employed method can be still further optimized. In addition, the described spin coating process allows for good homogeneity of the deposited layers by a fast and low cost method, which avoids vacuum-based techniques and complex pre-treatments of the Si surface.

2. Methods

An aqueous PEDOT:PSS dispersion at 1,3 % v/v (Sigma-Aldrich), presenting a sheet resistance below 100 (Ω/sq) and conductivities up to $\sigma=1000$ S/cm has been used as source of the conductive polymer in the composite layer. The SnO₂ and TiO₂ nanoparticles used as filler in the composite layer have been synthesized by hydrolysis. (100)-oriented Czochralski (CZ) Silicon wafers of *n*-type electrical conductivity with a nominal resistivity between 1-3 (Ω×cm) and thickness of 300 μm have been used in this work. A 40 nm thick layer of hydrogenated amorphous silicon (*a*-Si:H) has been deposited by plasma-enhanced chemical vapor deposition (PECVD) on the back side of the wafers as a reference passivation layer.

A thin layer of either non-functionalized PEDOT:PSS or PEDOT:PSS functionalized with rutile SnO₂ or TiO₂ nanoparticles have been deposited on top of the

Si substrates by spin coating. Ultra-sonication of the dispersion has been performed before the spin-coating in order to achieve a good dispersion of the nanomaterials in the PEDOT:PSS solution. After the spin-coating, a thermal annealing has been carried out on a hotplate at 120 °C for 20 minutes to evaporate water from PEDOT:PSS. The thickness of the films, 120 nm on average, was measured using an Alpha-Step profilometer.

X-ray diffraction (XRD) measurements were performed in a Philips X'Pert Pro diffractometer using Cu K_{α} radiation. High resolution transmission microscopy (HRTEM) was performed in a JEOL 3000 FEG electron microscope. For HRTEM measurements, the SnO₂ or TiO₂ nanopowders were dispersed in isopropanol and deposited on TEM grids.

Absorption spectra have been measured for bare PEDOT:PSS and hybrid PEDOT:PSS/nanoparticles deposited on glass substrates using the UV-Vis-NIR spectrophotometer (Ocean Optics QE65000). A photoluminescence (PL) imaging system was used for measuring the surface recombination at the Si surfaces. The effective charge carrier lifetime values were calculated from the PL intensity based on the quasi-steady state photoconductance (QSS-PC) measurements [21-23]. The setup was a LIS-R1 PL imaging setup from BT Imaging with an excitation wavelength of 808 nm and a constant illumination intensity of 4.2×10^{-2} W/cm². Optical micrographs have been acquired with a Leica DFC295 optical microscope. Compositional analysis by EDS was carried out using a Bruker AXS Quantax system working at 15kV and 1.5 nA in a Leica 440 Stereoscan SEM. μ -Raman spectroscopy has been performed in a confocal microscope (Horiba Jobin Yvon LabRAM HR 800) using an He-Ne red laser of 633nm wavelength. For the characterization of the solar device, a WACOM solar simulator with a short arc Xe lamp was used in order to simulate standard AM1.5 solar conditions. I-V measurements were carried out with a Keithley 4200-SCS .

3. Results and discussion

3.1 Inorganic nanomaterials functionalizing the PEDOT:PSS

SnO₂ and TiO₂ nanoparticles synthesized by hydrolysis method have been used as filler of the composite passivation layer consisting of PEDOT:PSS as a host. Prior to the study of the passivation properties of the composites, a study of the nanoparticles has been carried out. XRD measurements [Fig. 1a] confirm that the nanoparticles consist of cassiterite SnO₂ and TiO₂ anatase phase (hereinafter named as A-TiO₂). According to the Scherrer formula dimensions about 5-8 nm have been estimated for the nanoparticles. By thermal treatment at 1000 °C during 24 hours, the powders in anatase phase have been transformed into the rutile phase to be called hereafter as R-TiO₂. As a consequence of the thermal treatment grain growth was induced and the average size of the rutile nanoparticle is 50 nm, as estimated by the Scherrer formula.

Figure 1b displays HRTEM micrograph for SnO₂ nanoparticles that confirms high crystallinity of the as-grown nanoparticles, as well as their homogeneity and reduced dimensions. In this case, interplanar distances of 3.35 y 4.74 Å, corresponding to (110) y (001) planes in rutile SnO₂ respectively, are indicated in the image. FFT patterns along the [101] and [111] axes are marked as well in Figures 1c and 1d, respectively.

3.2 Si surface passivation

The charge carrier lifetimes have been measured by PL imaging for Si passivated by PEDOT:PSS from front side and by *a*-Si:H from back side. Figure 2 (a) and (b) shows the PL images acquired by illumination from the PEDOT:PSS or the *a*:Si-H sides that

gives the average lifetimes around 10 μs and 33 μs , respectively. Analysis shows that the PL images are more homogenous for illumination from *a*-Si:H side.

Dispersions of PEDOT:PSS and SnO₂ or TiO₂ nanoparticles in the concentration range from 0.25 to 5 wt% have been prepared following the method described in Refs [24-25]. The thus obtained hybridized PEDOT:PSS has been deposited on Si. Figures 3 (a)-(c) show the PL images and injection-level dependences of carrier lifetimes for Si passivated by PEDOT:PSS/SnO₂, PEDOT:PSS/A-TiO₂, and PEDOT:PSS/R-TiO₂ respectively. The homogeneous PL images are obtained for the illumination from the *a*-Si:H side [Fig. 3]. Analysis shows that the average charge carrier lifetime for functionalization of PEDOT:PSS with SnO₂ nanoparticles is clearly increased [Fig. 3a] by around one order of magnitude as compared to the value of bare PEDOT:PSS, while functionalization with A-TiO₂ nanoparticles provides the average lifetime of $\sim 30 \mu\text{s}$ [Fig. 3b]. Contrary to the case of A-TiO₂ nanoparticle composite, the use of R-TiO₂ nanoparticles significantly improves the average lifetime (see Fig. 3c), although the values of the SnO₂ composite are not reached. Regarding the homogeneity of the films and charge carriers lifetime, the best results have been also achieved by using SnO₂ as a filler, rather than A-TiO₂, and R-TiO₂.

A further analysis showed that the quality of the passivation mainly depends on the concentration of the nanoparticles in the initial dispersion, as confirmed by measurements of the charge carrier lifetime. The passivation properties have been systematically measured for the composite films as a function of the concentration of nanoparticles (0.25, 0.5, 1, 3, and 5 wt% in the starting dispersion). Figures 4a and 4b shows the dependence of the measured carrier lifetime on the concentration of SnO₂ and R-TiO₂ nanoparticles, respectively, which is not monotonic. The carrier lifetime, calculated by QSS-PC based on the PL intensity, increases with increasing the concentration of SnO₂ or R-TiO₂ at

smaller concentrations, and decreases at higher concentrations. Optimal concentrations of nanoparticles have been determined as 0.5 wt.% showing a maximum lifetime of 275 μs for SnO_2 , and 1.0 wt.% in the case of TiO_2 with the largest carrier lifetime of 160 μs . These results indicate that the initial concentration of nanoparticles is a crucial parameter to be controlled in order to achieve improved passivation performance. This also shows that the layers of PEDOT:PSS with SnO_2 nanoparticles provide better passivation performance of Si surface than bare PEDOT:PSS. The largest charge carrier lifetime achieved in this work is smaller than 2.41 ms [26-27] obtained by passivation with the stack $\text{a-SiO}_x\text{N}_y\text{:H/SiN}_x$. However, the stack is deposited by PECVD whereas the deposition process used in this work is low cost, fast and there is room for further enhancement of the lifetime.

In order to achieve deeper understanding of the improved passivation behavior achieved by using SnO_2 nanoparticles in the composite, the optical and compositional properties of the layers with the optimized concentration of SnO_2 nanoparticles (0.5 % wt) have been investigated and compared to the case of the best results using R- TiO_2 (1% wt.) and bare PEDOT:PSS. The films have been deposited by spin coating on glass substrates for the absorbance measurements; therefore the absorption spectrum from the glass substrate is also included as a reference. All samples show a high level of transparency in the visible range, as expected. As observed in Figure 5, where a comparison to the glass substrate is also shown, the optical absorption of the PEDOT:PSS and PEDOT:PSS/ SnO_2 or R- TiO_2 films in the visible range is lower than 10 %. Only high absorption is observed in the UV range. Since SnO_2 and R- TiO_2 are wide band gap oxides, upon functionalization of PEDOT:PSS with these nanoparticles the optical absorption properties of the hybrid material are not expected to significantly change, as shown in Figure 5. Hence, the optical transparency to the visible characteristic of the PEDOT:PSS

is slightly modified by adding SnO₂ or R-TiO₂ nanoparticles, which assures its suitability for use in devices requiring high transparency, while adding good passivation behavior. Besides, the observed improvement in absorption due to the presence of the nanoparticles in the polymer host could be beneficial for obtaining higher carrier generation levels in the device. Another advantage that should be considered in the future research, especially in the case of the bigger R-TiO₂ nanoparticles, is the light trapping effect produced by the light scattering at nanoparticles randomly embedded in a PEDOT layer. The recent work of Park et al. [28] shows that, although theoretically light harvesting by periodic structures can be better, random 100 nm sized TiO₂ nanoparticles in PEDOT show enhanced performance due to an increased optical path-length.

By EDS measurements, the chemical analysis of the PEDOT:PSS/SnO₂ or R-TiO₂ nanoparticles films was performed and carbon, silicon, oxygen, sulphur and tin or titanium were detected, as observed in the EDS spectra of Figure 6. Carbon and sulphur came from the PEDOT:PSS, oxygen from both polymer and nanoparticles, whereas tin or titanium came from the nanoparticles. EDS map confirms a high spatial homogeneity of the spin coated films (not shown here).

By using Raman spectroscopy, the structural configuration has been studied to achieve a better understanding of our system, as well as a fingerprint of the material, which forms our composites. In Figure 7a Raman spectra of bare PEDOT:PSS and SnO₂ 5% wt. or R-TiO₂ 5 % wt. doped PEDOT: PSS are shown. In the case of PEDOT:PSS its characteristic spectrum corresponding to benzoic structure can be seen, with the main band between 1400-1500 cm⁻¹, which corresponds to the stretching vibration of C_α=C_β on the five-member ring of PEDOT [29]. In particular, contribution from C-C inter-ring stretching (1258 cm⁻¹), single C-C stretching (1364 cm⁻¹), C-C symmetrical stretching (1441 cm⁻¹), C-C asymmetrical stretching (1510 cm⁻¹) and C-C antisymmetrical

stretching (1567 cm^{-1}) can be identified in Figure 7b. In the case of the PEDOT:PSS/nanoparticle films, these bands are also observed, as well as the peaks corresponding to rutile structure of the SnO_2 nanoparticles ($E_g=474\text{ cm}^{-1}$ and $A_{1g}=633\text{ cm}^{-1}$) or R- TiO_2 nanoparticles ($E_g=447\text{ cm}^{-1}$ and $A_{1g}=611\text{ cm}^{-1}$). In addition, the peak corresponding to crystalline silicon (520 cm^{-1}) from the substrate also appears in the Raman spectra. As observed in the Raman spectra of Figure 7b, the titanium oxide composite exhibits the main band of PEDOT:PSS around $1400\text{-}1500\text{ cm}^{-1}$, almost unchanged with respect to the bare PEDOT:PSS, whereas for the tin oxide composite this band is blurred out and shifted with respect to the bare PEDOT:PSS. Moreover, a shoulder at about 700 cm^{-1} can be observed in the spectrum from the PEDOT:PSS/ SnO_2 (Figure 7a) which can be associated to the symmetric C-S-C deformation, although activation of A_{2u} mode (705 cm^{-1}) in rutile SnO_2 cannot be excluded. This demonstrates that the properties of the composite film are not merely the addition of the properties of the single counterparts, moreover in the case of the tin oxide composite interactions between PEDOT:PSS and the tin oxide nanoparticles are revealed.

Metal oxide nanoparticles exhibit a charged surface in aqueous dispersions due to the complete coverage of the surface by hydroxyl groups [30]. The surface charge density depends on the nanoparticle size, pH and molar concentration of the dispersion [31]. The PEDOT:PSS/nanoparticle aqueous dispersion used as precursor in this study presents low pH values ($\text{pH}<2,5$) and molar concentrations and, therefore, under these conditions the nanoparticle surfaces are expected to be positively charged [32]. This positive charge density at the surface would help to trap electrons in the composite, which are the minority carriers in the hybrid layer hence improving the passivation of the Si/PEDOT:PSS interface. Furthermore, several studies [31-32] showed dependence of the surface charge density on nanoparticle size. This fact could be the origin of the charge-based passivation

mechanism observed in the present work, as rutile tin oxide nanoparticles present smaller size than the rutile titanium oxide nanoparticles exhibiting the former the best passivation results. Although these general observations are in agreement with our results for the composites showing good passivation results, surface properties characteristic from each semiconducting nanomaterial, such as different surface chemistry, interaction of surface defects with absorbed molecules and electronic properties should also play a role. Therefore, this could be responsible for the discrepancy observed for the results achieved for anatase nanoparticles with sizes under 10 nm [33-34] in comparison with the better performance of rutile 50 nm sized nanoparticles. As for example, Lira-Cantu and coworkers [34] show that the photovoltaic properties of TCO/TiO₂/polymer/Ag bi-layer solar cells is affected by the TiO₂ phase, being its rutile phase beneficial for long-term stability devices. From the study of different polymer/oxide interfaces it is argued that the higher amount of O_{vac} formed in anatase in comparison with rutile (which is also related to the higher conductivity and better photocatalytic properties of the anatase phase [35]), the higher amount of recombination centers can be expected in anatase in comparison with rutile-based devices reducing the free charges in the composite. In agreement with this observation our previous XPS and cathodoluminescence analysis of rutile and anatase nanoparticles grown by a liquid-mix technique show that oxygen vacancies are the dominant defect of anatase TiO₂ whereas a higher amount of Ti³⁺ defects are formed for rutile TiO₂ nanoparticles [36-37].

3.3 Pre-treatment of the Si surfaces prior to deposition and use of additives in the PEDOT dispersion

In order to achieve optimization of the passivation behavior, sensitivity of the results to the quality of processing of Si surface has been also performed. The larger

lifetimes, and hence better passivation behavior, has been achieved when no special HF cleaning of the Si wafer was performed.

In addition, Ethylene glycol (EG) has been used to enhance the dispersion of the nanoparticles and avoid aggregation during the spin coating, which results in a higher homogeneity of the deposited films. The use of EG could also improve the electrical conductivity of the polymer, due to alignment of the polymer chains. However, when no EG was added to the dispersion, no significant variations in the passivation behaviour were measured, while good homogeneity was still reached in the spin coated layers. There have been some studies about functionalizing PEDOT:PSS by different types of organic surfactants to enhance dispersion of the polymer on Si surface. In particular, Triton-X100 [38] as well as cationic and anionic surfactants [39] have been added. Ethylen glycol and dimethyl sulfoxide has been also added [40] into PEDOT:PSS to increase its electrical conductivity by defect minimization that allowed to achieve the efficiency of 13.3 %.

Therefore, in order to ease the spin-coating process, neither HF or RCA cleaning, nor EG additives have been used in this work. This issue makes attractive this surface passivation method, as the spin-coating technique has the enormous advantage over the existing vacuum-based techniques that involves low cost, easy and fast procedure, no complicated pre-treatments and deposition can be carried out at room temperature.

3.4 A hybrid organic/inorganic solar cell

In order to analyse the applicability of these hybrid composites, a photovoltaic device based on the PEDOT:PSS functionalized with SnO₂ and TiO₂ nanoparticles has been fabricated in the present study, following the standard procedure reported in the scientific literature [1, 6, 11, 41]. Figure 8a illustrates a scheme of the basic hybrid organic-Si solar cell built up in this work. Figures 8b and 8c show optical images of front

and backside of the developed solar cell, respectively. In the fabrication of this device Ag was used as front and rear ohmic contact. I-V measurements were carried out under dark or illumination conditions, as shown in Figure 9, where Figure 9a corresponds to the cell with bare PEDOT:PSS and Figure 9 (b) and (c) correspond to the PEDOT:PSS functionalized with SnO₂ 0.5 wt.% and R-TiO₂ 1 wt.% nanoparticles, respectively. A Xe short arc lamp, with an irradiance of 1 sun (~1000 Wm⁻²), was employed for the measurements under illumination. A Schottky behaviour was observed in the I-V curves, as expected. Illumination leads to the generation of a photocurrent as can be seen in Figure 9, especially in Figs. 9 (b) and (c), which demonstrates a potential photovoltaic behaviour. The obtained short-circuit current (I_{SC}) and open-circuit voltage (V_{OC}) values are higher when PEDOT:PSS was functionalized with nanoparticles. Values of 0.20 V (V_{OC}) and 0.0011 mA (I_{SC}), as well as a fill factor (FF) of 0.31 were estimated from the I-V curves acquired when using bare PEDOT:PSS, as a reference. Values of 0.29 V (V_{OC}) and 0.018 mA (I_{SC}) and a fill factor (FF) about 0.36 were achieved when using SnO₂ 0.5 wt.% in the hybrid film, while values of 0.23 V (V_{OC}) and 0.035 mA (I_{SC}) and a fill factor (FF) about 0.28 were achieved when using R-TiO₂ 1 wt%. Even when the efficiency of the developed device is low, as usually reported for similar hybrid cells, and taken into account that it can be clearly improved, these preliminary results indicate the potential applicability of the spin coated hybrid film in this field.

Conclusions

Surface passivation for *n*-type Si by PEDOT:PSS undoped or functionalized by semiconducting metal oxide nanoparticles has been studied. A strong enhancement of the surface passivation for *n*-Si is reported as a result of the functionalization of PEDOT:PSS

by SnO₂ and TiO₂ nanoparticles. The optimal concentration of the nanoparticles, defined as the concentration yielding the highest minority carrier lifetimes, has been determined to be 0.5% for SnO₂ and 1.0% for rutile TiO₂. A peak lifetime of 275 μs has been reached for the PEDOT-PSS/SnO₂. The functionalization of PEDOT:PSS with the nanoparticles only slightly changes its optical absorption and reflectance properties, as these properties are usually directly related to the concentration of the filler in the composite and the amount of nanoparticles used is limited under few percent. However reduced nanoparticle diameter as well as a strong coupling of tin oxide nanoparticles to PEDOT:PSS is observed as determined by Raman, which might be the origin of the enhanced passivation properties determined for these nanoparticles as compared to the titanium oxide ones and the reason to require 2 times less concentration of SnO₂ nanoparticles in the composite while achieving 2 times better lifetime results. The passivation of nanoparticles is reinforced by the chemical passivation of a native SiO₂ thin layer formed at the interface between the composite hybrid layer and the silicon surface, which eliminates the need of applying precleaning procedures to the silicon wafer reducing time, cost and being environmentally friendly. A simple solar cell device based on the spin coated hybrid composites have been developed and better photovoltaic behavior was achieved when using SnO₂ or R-TiO₂ nanoparticles in the polymer. When a high homogeneous hybrid layer is spin coated, it can be used as a substrate on top of which a new layer could be deposited in order to fabricate multilayer structures. Following this procedure layers with a concentration gradient of semiconducting oxide nanostructures in PEDOT:PSS can be fabricated, as well as multilayers with tuned optical properties, as an example, making use of the different properties achieved by doping and the combination of materials with different band gaps. This can widen the performance and applicability of these results in

the field of solar cells, and other optoelectronic devices, while keeping high homogeneity in the layers and involving low costs.

Acknowledgements. The work has been supported by the NILS “Sustainable oxide materials and nano-structures for energy related applications (SUSOX)” (008-ABELCM-2013) project, SIS Solcelletek Organisk-Si Hybrid project, MINECO/FEDER (MAT 2015-65274-R and MAT 2016-81720-REDC) projects, and New Indigo project 237643/E20. MGT and SZK thank Dr. J. H. Selj, R. Søndena, B. Thomassen, Ø. Nordseth from the Institute for Energy Technology, Norway, Professor Ellen Moons from Karlstad University, Sweden as well as Professor S. Senthilarasu from the University of Exeter, UK for practical help.

References

- (1) D. Zielke, A. Pazidis, F. Werner, J. Schmidt. Organic-Silicon Heterojunction Solar Cells on N-Type Silicon Wafers: The Backpedot Concept. *Solar Energy Mater. Solar Cells*. **131**, (2014), 110-116.
- (2) D. Zielke, C. Niehaves, W. Lövenich, A. Elschner, M. Hörteis, J. Schmidt. Organic-Silicon Solar Cells Exceeding 20% Efficiency. *Energy Proc.* **77**, (2015), 331-339.
- (3) A. M. Nardes, M. Kemerink, M. M. de Kok, E. Vinken, K. Maturova, R. A. J. Janssen. Conductivity, Work Function, and Environmental Stability of Pedot:Pss Thin Films Treated with Sorbitol. *Org. Electron.* **9**(5), (2008), 727-734.
- (4) L. Groenendaal, F. Jonas, D. Freitag, H. Pielartzik, J. R. Reynolds. Poly(3,4-Ethylenedioxythiophene) and Its Derivatives: Past, Present, and Future. *Adv. Mater.* **12**(7), (2000), 481-494.
- (5) S. Timpanaro, M. Kemerink, F. J. Touwslager, M. M. De Kok, S. Schrader. Morphology and Conductivity of Pedot/Pss Films Studied by Scanning-Tunneling Microscopy. *Chem. Phys. Lett.* **394**(4-6), (2004), 339-343.
- (6) J. Schmidt, V. Titova, D. Zielke. Organic-Silicon Heterojunction Solar Cells: Open-Circuit Voltage Potential and Stability. *Appl. Phys. Lett.* **103**(18), (2013), -.
- (7) P. Yu, C.-Y. Tsai, J.-K. Chang, C.-C. Lai, P.-H. Chen, Y.-C. Lai, P.-T. Tsai, M.-C. Li, H.-T. Pan, Y.-Y. Huang, C.-I. Wu, Y.-L. Chueh, S.-W. Chen, C.-H. Du, S.-F. Horng, H.-F. Meng. 13% Efficiency Hybrid Organic/Silicon-Nanowire Heterojunction Solar Cell Via Interface Engineering. *ACS Nano*. **7**(12), (2013), 10780-10787.
- (8) B. G. Lee, S. Li, G. von Gastrow, M. Yli-Koski, H. Savin, V. Malinen, J. Skarp, S. Choi, H. M. Branz. Excellent Passivation and Low Reflectivity with Atomic

- Layer Deposited Bilayer Coatings for N-Type Silicon Solar Cells. *Thin Solid Films*. **550**(0), (2014), 541-544.
- (9) D. Biro, W. Warta. Low Temperature Passivation of Silicon Surfaces by Polymer Films. *Solar Energy Mater. Solar Cells*. **71**(3), (2002), 369-374.
- (10) Y. Li, P. Fu, R. Li, M. Li, Y. Luo, D. Song. Ultrathin Flexible Planar Crystalline-Silicon/Polymer Hybrid Solar Cell with 5.68% Efficiency by Effective Passivation. *Appl. Surf. Sci.* **366**, (2016), 494-498.
- (11) L. He, C. Jiang, H. Wang, D. Lai, Rusli. High Efficiency Planar Si/Organic Heterojunction Hybrid Solar Cells. *Appl. Phys. Lett.* **100**(7), (2012), 073503.
- (12) R. Yang, T. Buonassisi, K. K. Gleason. Organic Vapor Passivation of Silicon at Room Temperature. *Adv. Mater.* **25**(14), (2013), 2078-2083.
- (13) F. Zhang, D. Liu, Y. Zhang, H. Wei, T. Song, B. Sun. Methyl/Allyl Monolayer on Silicon: Efficient Surface Passivation for Silicon-Conjugated Polymer Hybrid Solar Cell. *ACS Appl. Mater. Interfaces*. **5**(11), (2013), 4678-4684.
- (14) X. Yu, X. Shen, X. Mu, J. Zhang, B. Sun, L. Zeng, L. Yang, Y. Wu, H. He, D. Yang. High Efficiency Organic/Silicon-Nanowire Hybrid Solar Cells: Significance of Strong Inversion Layer. *Sci. Reports*. **5**, (2015), 17371.
- (15) J. Sheng, D. Wang, S. Wu, X. Yang, L. Ding, J. Zhu, J. Fang, P. Gao, J. Ye. Ideal Rear Contact Formed Via Employing a Conjugated Polymer for Si/Pedot:Pss Hybrid Solar Cells. *RSC Adv.* **6**(19), (2016), 16010-16017.
- (16) D. D. Fung, L. Qiao, W. C. Choy, C. Wang, E. Wei, F. Xie, S. He. Optical and Electrical Properties of Efficiency Enhanced Polymer Solar Cells with Au Nanoparticles in a Pedot–Pss Layer. *J. Mater. Chem. A*. **21**(41), (2011), 16349-16356.

- (17) W.-J. Yoon, K.-Y. Jung, J. Liu, T. Duraisamy, R. Revur, F. L. Teixeira, S. Sengupta, P. R. Berger. Plasmon-Enhanced Optical Absorption and Photocurrent in Organic Bulk Heterojunction Photovoltaic Devices Using Self-Assembled Layer of Silver Nanoparticles. *Solar Energy Mater. Solar Cells.* **94**(2), (2010), 128-132.
- (18) S.-J. Wang, H.-H. Park. Study of Pedot:Pss-Sno₂ Nanocomposite Film as an Anode for Polymer Electronics. *J. Electroceram.* **18**(1), (2007), 161-165.
- (19) Y. Liu, D. Sun, S. Askari, J. Patel, M. Macias-Montero, S. Mitra, R. Zhang, W.-F. Lin, D. Mariotti, P. Maguire. Enhanced Dispersion of Tio₂ Nanoparticles in a Tio₂/Pedot:Pss Hybrid Nanocomposite Via Plasma-Liquid Interactions. *Sci. Reports.* **5**, (2015), 15765.
- (20) K. H. Yoo, K. S. Kang, Y. Chen, K. J. Han, K. Jaehwan. The Tio₂ Nanoparticle Effect on the Performance of a Conducting Polymer Schottky Diode. *Nanotechnol.* **19**(50), (2008), 505202.
- (21) T. Trupke, R. Bardos, M. Schubert, W. Warta. Photoluminescence Imaging of Silicon Wafers. *Appl. Phys. Lett.* **89**(4), (2006), 044107.
- (22) T. Trupke, R. Bardos, M. Abbott. Self-Consistent Calibration of Photoluminescence and Photoconductance Lifetime Measurements. *Appl. Phys. Lett.* **87**(18), (2005), 184102.
- (23) T. U. Nærland, H. Angelskår, M. Kirkengen, R. Søndena, E. S. Marstein. The Role of Excess Minority Carriers in Light Induced Degradation Examined by Photoluminescence Imaging. *J. Appl. Phys.* **112**(3), (2012), 033703.
- (24) M. García-Tecedor, G. C. Vásquez, M. González-Taeño, D. Maestre, A. Cremades, J. Ramírez-Castellanos, J. Piqueras, J. M. González-Calbet, S. Karazhanov, H. Haug, C. G. You, a. E. S. Marstein. *Organic-Inorganic Hybrid Material and Method for Silicon Surface Passivation*. US Patent, 2016.

- (25) M. García-Tecedor, G. C. Vásquez, M. González-Taeño, D. Maestre, A. Cremades, J. Ramírez-Castellanos, J. Piqueras, J. M. González-Calbet, S. Karazhanov, H. Haug, C. G. You, E. S. Marstein. *Material Híbrido Orgánico-Inorgánico Y Método Para Pasivación De Superficie De Silicio*. US Patent, 2016.
- (26) X. Cheng, H. Haug, M. D. Sabatino, J. Zhu, E. S. Marstein. Electronic Properties of a-SiO_xN_y:H/Si_n Stacks for Surface Passivation of P-Type Crystalline Si Wafers. *IEEE J. Photovoltaics*. **6**(5), (2016), 1103-1108.
- (27) B. Hallam, M. Abbott, T. Nærland, S. Wenham. Fast and Slow Lifetime Degradation in Boron - Doped Czochralski Silicon Described by a Single Defect. *Phys. Stat. Solidi (RRL)*. **10**(7), (2016), 520-524.
- (28) Y. Park, L. Müller-Meskamp, K. Vandewal, K. Leo. Pedot: Pss with Embedded TiO₂ Nanoparticles as Light Trapping Electrode for Organic Photovoltaics. *Appl. Phys. Lett.* **108**(25), (2016), 253302.
- (29) N. Semaltianos, S. Logothetidis, N. Hastas, W. Perrie, S. Romani, R. Potter, G. Dearden, K. Watkins, P. French, M. Sharp. Modification of the Electrical Properties of Pedot: Pss by the Incorporation of ZnO Nanoparticles Synthesized by Laser Ablation. *Chem. Phys. Lett.* **484**(4), (2010), 283-289.
- (30) A. Dhakshinamoorthy, S. Navalon, M. Alvaro, H. Garcia. Metal Nanoparticles as Heterogeneous Fenton Catalysts. *ChemSusChem*. **5**(1), (2012), 46-64.
- (31) J. P. Holmberg, E. Ahlberg, J. Bergenholtz, M. Hassellöv, Z. Abbas. Surface Charge and Interfacial Potential of Titanium Dioxide Nanoparticles: Experimental and Theoretical Investigations. *J. Colloid Interface Sci.* **407**, (2013), 168-176.
- (32) N. Wang, C. Hsu, L. Zhu, S. Tseng, J.-P. Hsu. Influence of Metal Oxide Nanoparticles Concentration on Their Zeta Potential. *J. Colloid Interface Sci.* **407**, (2013), 22-28.

- (33) G. D. Panagiotou, T. Petsi, K. Bourikas, C. S. Garoufalis, A. Tsevis, N. Spanos, C. Kordulis, A. Lycourghiotis. Mapping the Surface (Hydr) Oxo-Groups of Titanium Oxide and Its Interface with an Aqueous Solution: The State of the Art and a New Approach. *Adv. Colloid Interface Sci.* **142**(1), (2008), 20-42.
- (34) M. Lira-Cantu, A. Chafiq, J. Faissat, I. Gonzalez-Valls, Y. Yu. Oxide/Polymer Interfaces for Hybrid and Organic Solar Cells: Anatase Vs. Rutile Tio 2. *Solar Energy Mater. Solar Cells.* **95**(5), (2011), 1362-1374.
- (35) A. A. Bonapasta, F. Filippone, G. Mattioli, P. Alippi. Oxygen Vacancies and Oh Species in Rutile and Anatase Tio 2 Polymorphs. *Catalysis Today.* **144**(1), (2009), 177-182.
- (36) G. C. Vásquez, M. A. Peche-Herrero, D. Maestre, A. Gianoncelli, J. Ramírez-Castellanos, A. Cremades, J. M. González-Calbet, J. Piqueras. Laser-Induced Anatase-to-Rutile Transition in Tio2 Nanoparticles: Promotion and Inhibition Effects by Fe and Al Doping and Achievement of Micropatterning. *J. Phys. Chem. C.* **119**(21), (2015), 11965-11974.
- (37) G. C. Vásquez, M. A. Peche-Herrero, D. Maestre, A. Cremades, J. Ramírez-Castellanos, J. M. González-Calbet, J. Piqueras. Effects of Transition Metal Doping on the Growth and Properties of Rutile Tio2 Nanoparticles. *J. Phys. Chem. A.* **117**(4), (2013), 1941-1947.
- (38) J. P. Thomas, L. Zhao, M. Abd-Ellah, N. F. Heinig, K. T. Leung. Interfacial Micropore Defect Formation in Pedot:Pss-Si Hybrid Solar Cells Probed by Tof-Sims 3d Chemical Imaging. *Anal. Chem.* **85**(14), (2013), 6840-6845.
- (39) B. Fan, Y. Xia, J. Ouyang, editors; Proc. SPIE 7415 Organic Light Emitting Materials and Devices XIII; 2009; 74151Q-74151Q-74159.

- (40) J. P. Thomas, K. T. Leung. Defect-Minimized Pedot:Pss/Planar-Si Solar Cell with Very High Efficiency. *Adv. Funct. Mater.* **24**(31), (2014), 4978-4985.
- (41) S. Jäckle, M. Mattiza, M. Liebhaber, G. Brönstrup, M. Rommel, K. Lips, S. Christiansen. Junction Formation and Current Transport Mechanisms in Hybrid N-Si/Pedot:Pss Solar Cells. *Sci. Rep.* **5**, (2015), 13008.

Figure captions:

Figure 1. (a) XRD of SnO₂ and A-TiO₂ nanoparticles, (b) HRTEM image and electron diffraction patterns of SnO₂ nanoparticles.

Figure 2. PL image of passivated Si wafer illuminated from (a) PEDOT:PSS and (b) *a*-Si:H sides.

Figure 3. PL images of a composite sample containing (a) SnO₂ nanoparticles in 5wt.% concentration, (b) A-TiO₂ nanoparticle in 5 wt.% and (c) R-TiO₂ nanoparticles in a 5 wt.% obtained by illumination from the PEDOT:PSS or from the *a*-Si:H side. The corresponding QSS-PCC measurements are also shown.

Figure 4. Carrier lifetime as a function of the concentration of (a) SnO₂ nanoparticles and (b) R-TiO₂ nanoparticles.

Figure 5. Absorption spectra of bare PEDOT:PSS and composite films with SnO₂ (0.5 % wt.) or R-TiO₂ (1 % wt.) deposited on glass. Absorption spectrum from glass is also shown for comparison.

Figure 6. EDS spectra acquitted on layers formed by PEDOT:PSS and SnO₂ nanoparticles (5 % wt.) and R-TiO₂ nanoparticles (5% wt.).

Figure 7. (a) Raman spectra of PEDOT: PSS (black line), PEDOT: PSS with SnO₂ nanoparticles 5 wt%. (blue line) and PEDOT: PSS with R-TiO₂ 5 wt% (red line). (b) Raman spectra for the samples in the region between 1000 and 1800 cm⁻¹, where the characteristic PEDOT: PSS benzoic structure is located.

Figure 8. (a) Design of the photovoltaic device with hybrid emitter. Images of the (a) front and (b) back side of the solar cell model.

Figure 9. Current-voltage dependence under dark and illumination for (a) bare PEDOT, (b) PEDOT:PSS/SnO₂ 0.5 wt% and (c) PEDOT:PSS/TiO₂ 1 wt%.

Figures:

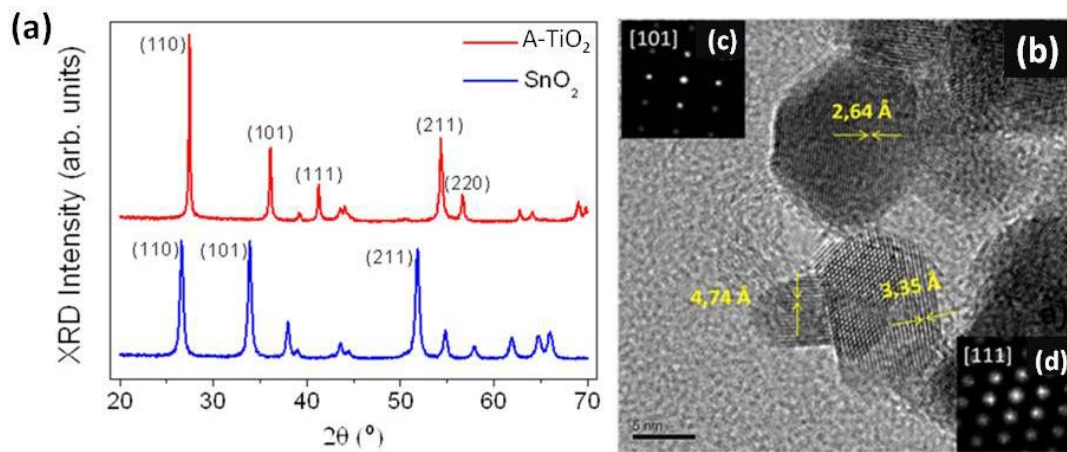


Figure 1

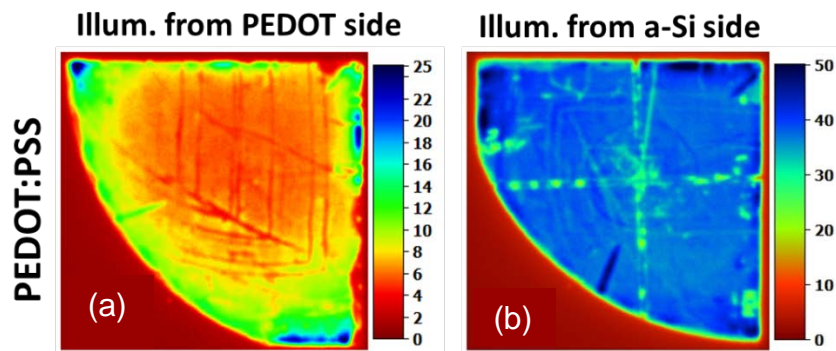


Figure 2

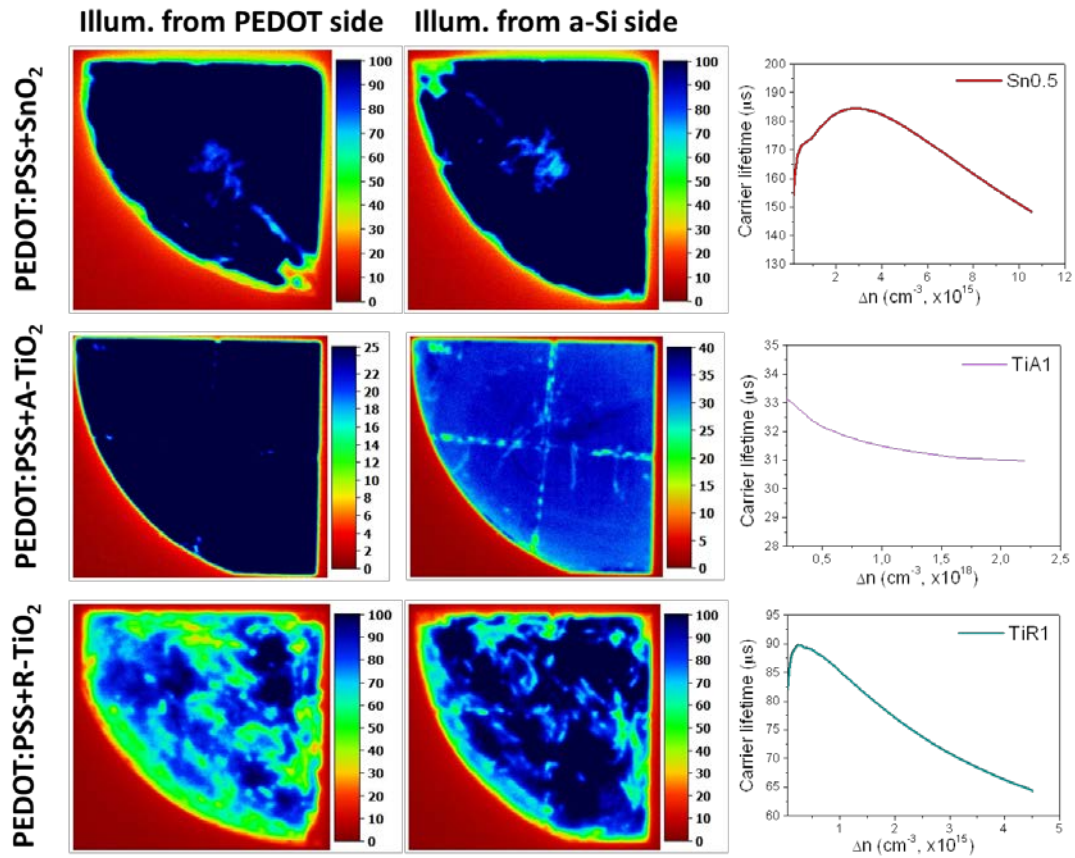


Figure 3

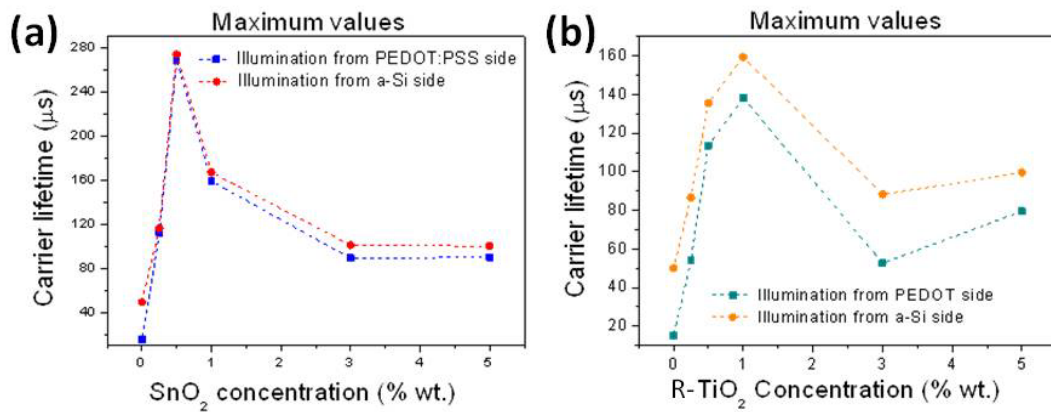


Figure 4

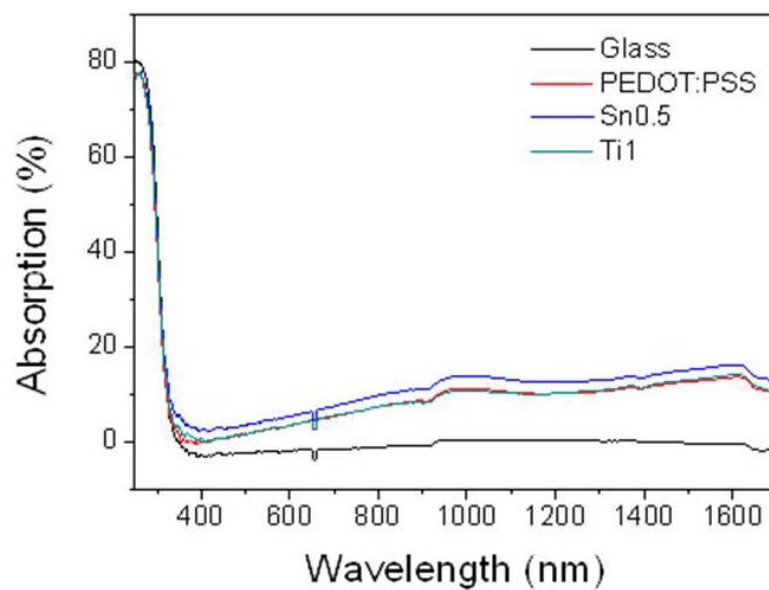


Figure 5

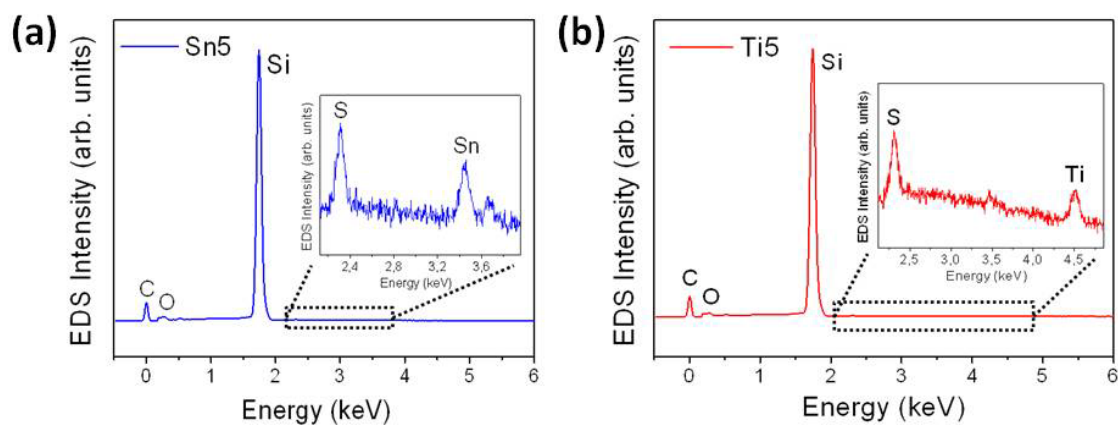


Figure 6

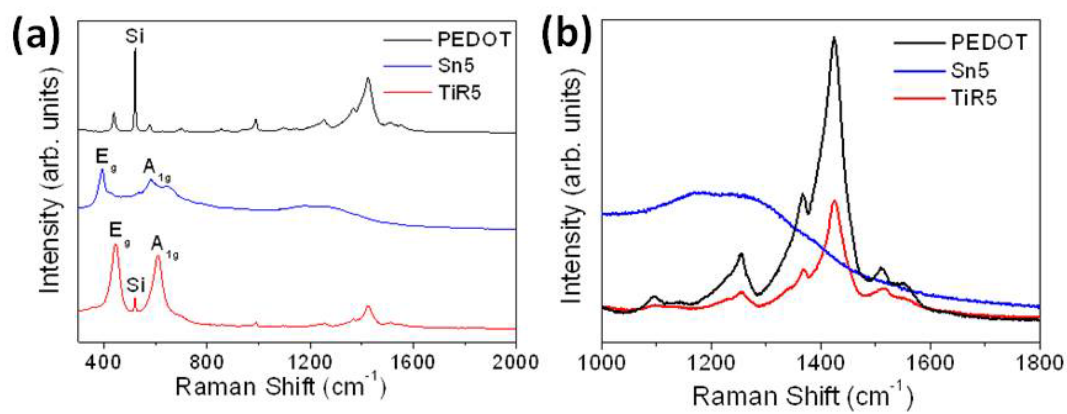


Figure 7

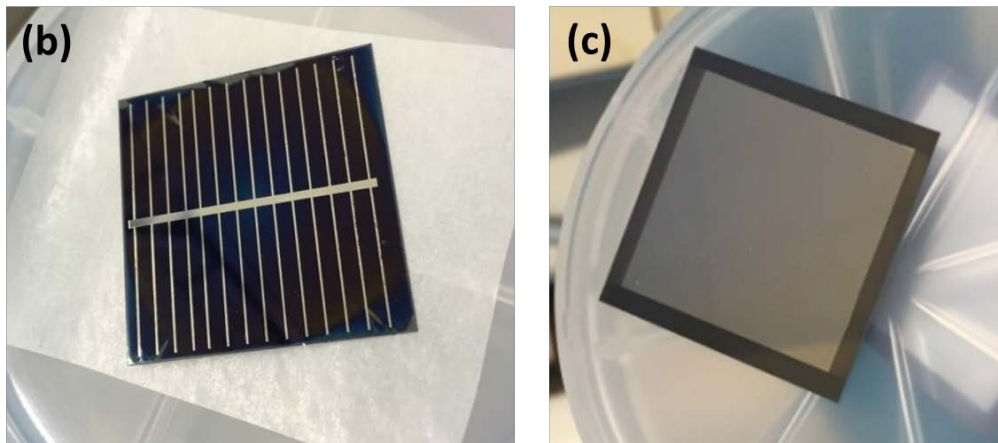
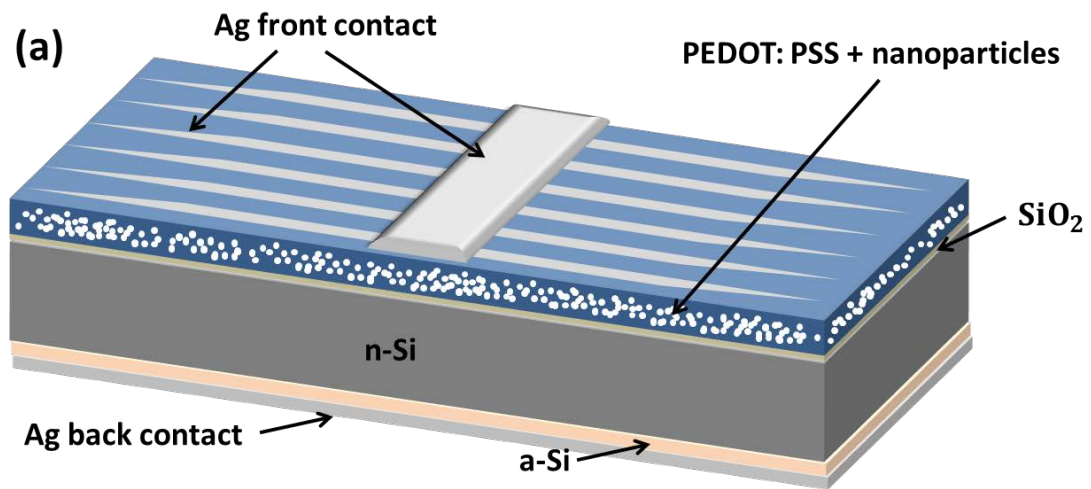


Figure 8

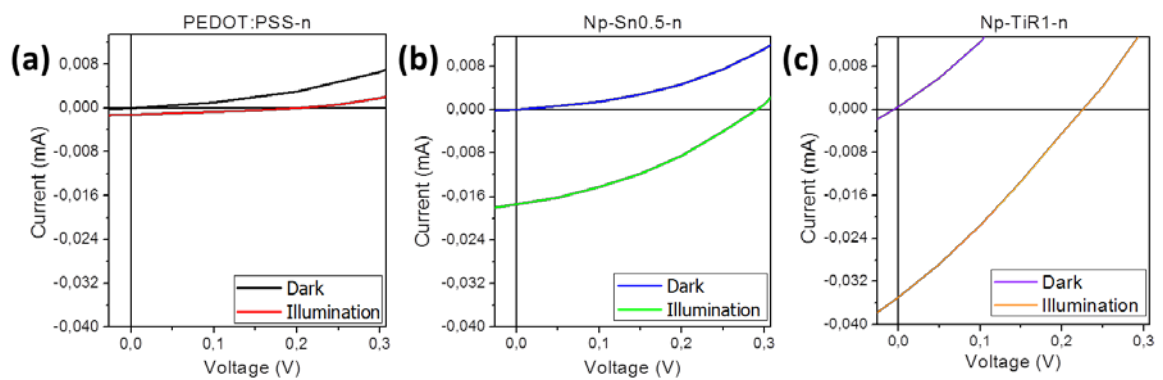


Figure 9